INTERNATIONAL JOURNAL FOR NUMERICAL METHODS IN FLUIDS
Int. J. Numer. Meth. Fluids 2009; **61**:848–863
Published online 16 December 2008 in Wiley InterScience (www.interscience.wiley.com). DOI: 10.1002/fld.1978

A lattice Boltzmann method for solute transport

Jian Guo Zhou*, †

Department of Engineering, University of Liverpool, Liverpool L69 3GQ, U.K.

SUMMARY

A lattice Boltzmann method is developed for solute transport. Proper expressions for the local equilibrium distribution functions enable the method to be formulated on rectangular lattice with the same simple procedure as that on a square lattice. This provides an additional advantage over a lattice Boltzmann method on a square lattice for problems characterized by dominant phenomenon in one direction and relatively weak in another such as solute transport in shear flow over a narrow channel, where the problems can efficiently be approached with fine and coarse meshes, respectively, resulting in more efficient algorithm. The stability conditions are also described. The proposed method on a square lattice is naturally recovered when a square lattice is used. It is verified by solving four tests and compared with the analytical/exact solutions. They are in good agreement, demonstrating that the method is simple, accurate and robust for solute transport. Copyright © 2008 John Wiley & Sons, Ltd.

Received 29 June 2007; Revised 31 March 2008; Accepted 8 November 2008

KEY WORDS: rectangular lattice; lattice Boltzmann method; solute transport; advection–diffusion equation; mathematical model; numerical method

1. INTRODUCTION

With the success of the lattice Boltzmann method for fluid flows, the method has been used in many different areas [1], demonstrating its efficiency, potential and capability. In recent years, the lattice Boltzmann method has already been far beyond its original application for fluid flows and been regarded as a novel numerical method for other problems. For example, Xu *et al.* [2] modelled molten carbonate fuel cell performance with lattice Boltzmann method. Zhou [3] developed a lattice Boltzmann model for groundwater flows. Ni *et al.* [4] investigated the lattice Boltzmann method for the statistical evolution of numerous microvoids under high stress triaxiality. Ghai *et al.* [5] used the lattice Boltzmann method to simulate the transient thermal response of a nanoscale hot spot in solids.

*Correspondence to: Jian Guo Zhou, Brodie Tower, Brownlow Street, Liverpool L69 3GQ, U.K.
†E-mail: j.g.zhou@liverpool.ac.uk

The lattice Boltzmann method is being improved and further developed. van der Sman [6] studied the characteristics of the lattice Boltzmann method fixing the single relaxation time to one and proposed a finite Boltzmann scheme. Rohde *et al.* [7] proposed a local grid refinement technique for the lattice Boltzmann method, allowing the method to be used from coarse to fine grid cells and vice versa. The restriction of the method to rectangular or square lattice has been investigated. van der Sman and Ernst [8] proposed a convection–diffusion lattice Boltzmann scheme for irregular lattices without need for interpolation. Later, van der Sman [9] extended the scheme for diffusion problem on unstructured triangular grids. Chew *et al.* [10] developed a lattice Boltzmann method on irregular lattices by transforming the lattice Boltzmann equation into a differential form. Wu *et al.* [11] used interpolation technique to solve the lattice Boltzmann equation on non-uniform grids. Zhang *et al.* [12] presented a lattice Boltzmann model for advection–dispersion equation on rectangular lattice by use of both weighing factors in the calculation of the macroscopic quantity and more than three directionally dependent relaxation times.

In the literature, there are lattice Boltzmann methods available for solution of the advection–diffusion equation for solute transport, most of which are based on the standard hexagonal/square lattices [13–15]. Since a model with square lattices usually provides not only easier treatment of boundary conditions, but also more accurate results than that with hexagonal lattices [16, 17], square lattices become preferred in lattice Boltzmann simulations. Although Zhang *et al.* [12] developed a lattice Boltzmann model for solution of the equation on rectangular lattice, the use of at least three directionally dependent relaxation times makes the procedure more complex than the standard method. Thus, in this paper, a simple lattice Boltzmann model for solute transport on a rectangular lattice is proposed in a novel way. The method is effectively the same as that on a square lattice. It is a natural extension of the lattice Boltzmann method on square lattice to rectangular lattice. The only difference lies in embedding the feature of a rectangular lattice in the proper local equilibrium distribution functions on a square lattice with least modification. When a square lattice is applied, the proposed method on a square lattice is naturally recovered without any additional treatment. It is validated by solving four benchmark problems and the results are compared with analytical/exact solutions.

2. LATTICE BOLTZMANN METHOD

In this section, the governing equation for solute transport is introduced first. Then the lattice Boltzmann equation is described with proper expressions for the local equilibrium distribution functions on a rectangular lattice. Next the recovery of the advection–diffusion equation from the lattice Boltzmann equation is shown in detail. In addition, the boundary conditions are described. Finally, the stability conditions are discussed.

2.1. Solute transport

The transport of solute or concentration is described with the advection–diffusion equation in environmental hydraulics

$$\frac{\partial C}{\partial t}+\frac{\partial (u_i C)}{\partial x_i}=\frac{\partial}{\partial x_i}\left(D_i \frac{\partial C}{\partial x_i}\right) \tag{1}$$

DOI: 10.1002/fld

where C is the concentration, t the time, D_i the dispersion coefficient in i direction, u_i the fluid velocity, x_i the Cartesian coordinate in i direction and repeated index i is the Einstein summation convention, meaning a summation over the space coordinates. Such a convention is used throughout the paper.

2.2. *Lattice Boltzmann equation*

A lattice Boltzmann equation with the BGK collision operator is

$$f_\alpha(\mathbf{x}+\mathbf{e}_\alpha\Delta t, t+\Delta t)-f_\alpha(\mathbf{x},t)=-\frac{1}{\tau}(f_\alpha-f_\alpha^{\mathrm{eq}}) \tag{2}$$

in which f_α is the distribution function of particles, f_α^{eq} the local equilibrium distribution function, Δt the time step, $\mathbf{e}_\alpha$ the vector of the particle speed, τ the single relaxation time [18] and $\mathbf{x}$ the space vector defined by the Cartesian coordinate system, i.e. $\mathbf{x}=(x, y)$ in 2D space and $\mathbf{x}=(x, y, z)$ for 3D, where x and y stand for horizontal directions and z for vertical.

For simplicity without loss of generality, we may restrict the following description to the 2D situation and the similar procedure can be applied to the 3D case (A 3D lattice Boltzmann model for solute transport is given in the Appendix). Since there is only one scalar variable C to determine, the 5-speed rectangular lattice including a rest particle would be sufficient to simulate the solute transport, which is shown in Figure 1. The vector of the particle speed $\mathbf{e}_\alpha$ is defined by

$$\mathbf{e}_\alpha=\begin{cases}(0,0), & \alpha=0\\ e_x\left[\cos\dfrac{(\alpha-1)\pi}{2}, \sin\dfrac{(\alpha-1)\pi}{2}\right], & \alpha=1 \text{ and } 3\\ e_y\left[\cos\dfrac{(\alpha-1)\pi}{2}, \sin\dfrac{(\alpha-1)\pi}{2}\right], & \alpha=2 \text{ and } 4\end{cases} \tag{3}$$

where

$$e_x=\Delta x/\Delta t, \quad e_y=\Delta y/\Delta t \tag{4}$$

and Δx is the lattice size in the x direction and Δy in the y direction.

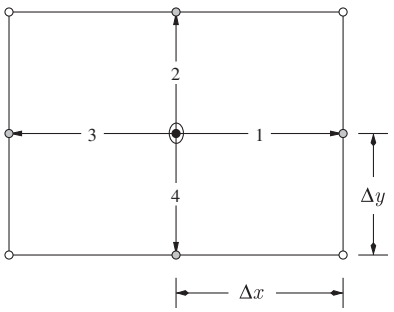

Figure 1. 5-velocity rectangular lattice.

DOI: 10.1002/fld

Now we define the concentration C in the distribution functions as

$$C(\mathbf{x},t)=\sum_{\alpha} f_{\alpha}(\mathbf{x},t) \tag{5}$$

which is the macroscopic quantity to be determined. Only if a suitable expression for the local equilibrium distribution function f_{α}^{eq} is defined, can the concentration resulted from the lattice Boltzmann equation (2) be the solution to Equation (1).

In the literature, there are some researches on choice of the equilibrium distribution functions in the lattice Boltzmann method for solution to the advection–diffusion equations. Dawson *et al.* [19] used a simple expression for the equilibrium distribution functions, which had the drawback that the same local equilibrium distribution function was applied to the rest particle as that to the particles else. Zhang *et al.* [12] retained the linear parts of the equilibrium distribution functions for the lattice Boltzmann method to solve the Navier–Stokes equation together with an additional function to avoid zero in the denominator as the equilibrium distribution functions. van der Sman and Ernst [20] used similar equilibrium distribution functions to that for the Navier–Stokes equations and the procedure is complicated.

In order to develop a simple lattice Boltzmann method on the rectangular lattice shown in Figure 1, we introduce the three following general constraints on f_{α}^{eq}:

$$\sum_{\alpha} f_{\alpha}^{\mathrm{eq}}=C \tag{6}$$

$$\sum_{\alpha} e_{\alpha i} f_{\alpha}^{\mathrm{eq}}=u_i C \tag{7}$$

$$\sum_{\alpha} e_{\alpha i} e_{\alpha j} f_{\alpha}^{\mathrm{eq}}=\lambda_i e_x e_y C \delta_{ij}=\begin{cases}\lambda_x e_x e_y C, & i=j=x\\ \lambda_y e_x e_y C, & i=j=y\end{cases} \tag{8}$$

where δ_{ij} is the Kronecker delta function defined as

$$\delta_{ij}=\begin{cases}0, & i\neq j\\ 1, & i=j\end{cases} \tag{9}$$

and λ_i is a constant, representing a dimensionless physical dispersion in the i direction as defined by Equation (27); in particular, λ_x and λ_y are the dimensionless physical dispersion coefficients in the x and y directions, respectively.

Based on the constraints (6)–(8) and the lattice symmetry, f_{α}^{eq} can be expressed in the following simple equation:

$$f_{\alpha}^{\mathrm{eq}}=\begin{cases}\left(1-\dfrac{\lambda_y e_x^2+\lambda_x e_y^2}{e_x e_y}\right)C, & \alpha=0\\ \left(\dfrac{1}{2}\dfrac{e_y}{e_x}\lambda_x+\dfrac{e_{\alpha i}u_i}{2e_x^2}\right)C, & \alpha=1 \text{ and } 3\\ \left(\dfrac{1}{2}\dfrac{e_x}{e_y}\lambda_y+\dfrac{e_{\alpha i}u_i}{2e_y^2}\right)C, & \alpha=2 \text{ and } 4\end{cases} \tag{10}$$

DOI: 10.1002/fld

It should be noted that Equations (5) and (6) together form a conservation condition as

$$\sum_{\alpha} f_{\alpha} = \sum_{\alpha} f_{\alpha}^{\mathrm{eq}} \tag{11}$$

If $\Delta x = \Delta y$ or $e_x = e_y$, Equation (10) becomes the local equilibrium distribution function for the lattice Boltzmann method on a square lattice.

2.3. Recovery of the advection–diffusion equation

The Chapman–Enskog expansion is used to prove that the concentration calculated from Equation (5) is the solution to the advection–diffusion equation (1) for solute transport, i.e. the macroscopic equation (1) can be derived from Equation (2). For this, we assume that Δt is small and equal to ε

$$\Delta t = \varepsilon \tag{12}$$

Substitution of Equation (12) into Equation (2) leads to

$$f_{\alpha}(\mathbf{x} + \mathbf{e}_{\alpha}\varepsilon, t + \varepsilon) - f_{\alpha}(\mathbf{x}, t) = -\frac{1}{\tau}(f_{\alpha} - f_{\alpha}^{\mathrm{eq}}) \tag{13}$$

Taking a Taylor expansion to the left-hand side of the above equation in time and space around point $(\mathbf{x}, t)$, we have

$$\varepsilon\left(\frac{\partial}{\partial t} + e_{\alpha j}\frac{\partial}{\partial x_j}\right) f_{\alpha} + \frac{1}{2}\varepsilon^2\left(\frac{\partial}{\partial t} + e_{\alpha j}\frac{\partial}{\partial x_j}\right)^2 f_{\alpha} + \mathcal{O}(\varepsilon^3) = -\frac{1}{\tau}(f_{\alpha} - f_{\alpha}^{\mathrm{eq}}) \tag{14}$$

According to the Chapman–Enskog expansion, f_{α} can be expressed as

$$f_{\alpha} = f_{\alpha}^{(0)} + \varepsilon f_{\alpha}^{(1)} + \varepsilon^2 f_{\alpha}^{(2)} + \mathcal{O}(\varepsilon^3) \tag{15}$$

Equation (14) to order ε^0 is

$$f_{\alpha}^{(0)} = f_{\alpha}^{\mathrm{eq}} \tag{16}$$

to order ε

$$\left(\frac{\partial}{\partial t} + e_{\alpha j}\frac{\partial}{\partial x_j}\right) f_{\alpha}^{(0)} = -\frac{1}{\tau} f_{\alpha}^{(1)} \tag{17}$$

and to order ε^2

$$\left(\frac{\partial}{\partial t} + e_{\alpha j}\frac{\partial}{\partial x_j}\right) f_{\alpha}^{(1)} + \frac{1}{2}\left(\frac{\partial}{\partial t} + e_{\alpha j}\frac{\partial}{\partial x_j}\right)^2 f_{\alpha}^{(0)} = -\frac{1}{\tau} f_{\alpha}^{(2)} \tag{18}$$

Substitution of Equation (17) into the above equation gives

$$\left(1 - \frac{1}{2\tau}\right)\left(\frac{\partial}{\partial t} + e_{\alpha j}\frac{\partial}{\partial x_j}\right) f_{\alpha}^{(1)} = -\frac{1}{\tau} f_{\alpha}^{(2)} \tag{19}$$

From Equation (17) + Equation (19) $\times\varepsilon$, we have

$$\left(\frac{\partial}{\partial t} + e_{\alpha j}\frac{\partial}{\partial x_j}\right) f_{\alpha}^{(0)} + \varepsilon\left(1 - \frac{1}{2\tau}\right)\left(\frac{\partial}{\partial t} + e_{\alpha j}\frac{\partial}{\partial x_j}\right) f_{\alpha}^{(1)} = -\frac{1}{\tau}(f_{\alpha}^{(1)} + \varepsilon f_{\alpha}^{(2)}) \tag{20}$$

DOI: 10.1002/fld

Now summing Equation (20) over all the directions and simplifying with the following relations,

$$\sum_{\alpha} f_{\alpha}^{(1)} = \sum_{\alpha} f_{\alpha}^{(2)} = 0 \tag{21}$$

and

$$\frac{\partial}{\partial t} \sum_{\alpha} f_{\alpha}^{(1)} = 0 \tag{22}$$

due to the conservation condition (11), provide

$$\frac{\partial}{\partial t} \sum_{\alpha} f_{\alpha}^{(0)} + \frac{\partial}{\partial x_j} \sum_{\alpha} e_{\alpha j} f_{\alpha}^{(0)} + \varepsilon \left(1 - \frac{1}{2\tau}\right) \frac{\partial}{\partial x_j} \sum_{\alpha} e_{\alpha j} f_{\alpha}^{(1)} = 0 \tag{23}$$

Substitution of Equation (17) into the above equation leads to

$$\frac{\partial}{\partial t} \sum_{\alpha} f_{\alpha}^{(0)} + \frac{\partial}{\partial x_i} \sum_{\alpha} e_{\alpha i} f_{\alpha}^{(0)} = \varepsilon \left(\tau - \frac{1}{2}\right) \frac{\partial}{\partial x_i} \sum_{\alpha} \left(e_{\alpha i} e_{\alpha j} \frac{\partial f_{\alpha}^{(0)}}{\partial x_j} \right) + \varepsilon \left(\tau - \frac{1}{2}\right) \frac{\partial}{\partial x_i} \sum_{\alpha} \left(e_{\alpha i} \frac{\partial f_{\alpha}^{(0)}}{\partial t} \right) \tag{24}$$

The last term on the right-hand side of the above equation is smaller compared with the first. It can be omitted and treated as a truncation error [12]. After substituting Equations (6) and (7) into the above equation with reference to Equation (16), an evaluation of the terms on the right-hand side using Equation (10) results in

$$\frac{\partial C}{\partial t} + \frac{\partial (u_i C)}{\partial x_i} = \frac{\partial}{\partial x_i} \left[\lambda_i \varepsilon \left(\tau - \frac{1}{2}\right) e_x e_y \frac{\partial C}{\partial x_i} \right] \tag{25}$$

If we set

$$\lambda_i \varepsilon (\tau - \tfrac{1}{2}) e_x e_y = D_i \tag{26}$$

then Equation (25) is just the governing equation (1) for solute transport. Notice $\varepsilon = \Delta t$ from Equation (12), rearranging Equation (26) gives λ_i,

$$\lambda_i = \frac{D_i}{\Delta t (\tau - \frac{1}{2}) e_x e_y} \tag{27}$$

In general, there are two boundary conditions for solute transport, gradient of concentration is zero and concentration is known. In the proposed model, zero gradient in distribution function can be used for the former boundary condition and bounce-back scheme can be used for the latter, e.g. unknown f_{α} is decided by

$$f_{\alpha} = \begin{cases} f_{\alpha+2}, & \alpha = 1 \text{ and } 2 \\ f_{\alpha-2}, & \alpha = 3 \text{ and } 4 \end{cases} \tag{28}$$

DOI: 10.1002/fld

In addition, a periodic boundary condition may be used to simulate long domain, e.g. for infinite domain in the x direction, the following conditions are used:

$$f_1|_{x=0} = f_3|_{x=L} \tag{29}$$

and

$$f_3|_{x=L} = f_1|_{x=0} \tag{30}$$

where L is channel length.

2.4. Stability conditions

The stability conditions can be similarly obtained following the procedure described by Zhou in the model for groundwater flows [3]. Since the concentration is always non-negative, it requires a positive value for the local equilibrium distribution functions. It is easily seen that from Equation (10) all the local equilibrium distribution functions are always positive except for f_0^{eq}; hence to ensure $f_0^{\mathrm{eq}}>0$, we require

$$\lambda_y e_x^2 + \lambda_x e_y^2 < e_x e_y \tag{31}$$

With reference to Equation (27), the above condition (31) can be rewritten as

$$\Delta t < \frac{(\tau - \frac{1}{2})\Delta x^2 \Delta y^2}{D_x \Delta y^2 + D_y \Delta x^2} \tag{32}$$

Since all Δt, Δx, Δy, D_x and D_y are always positive, Equation (32) can be true with proper values for Δt and τ only if

$$\tau > \tfrac{1}{2} \tag{33}$$

which is a basic rule to choose τ in the lattice Boltzmann equation (2) and consistent with the requirement of a positive viscosity in the lattice Boltzmann method for the Navier–Stokes equations.

Although the discussed requirements (32) and (33) are not sufficient conditions for stability, practical computations have shown that the method is often stable if they are satisfied in numerical solutions.

3. VERIFICATION

The method is applied to solve four test problems. The results are compared with the analytical/exact solutions to demonstrate its potential, capability and accuracy.

3.1. 1D solute transport within short distance

The first test is that a conservative solute is introduced into a saturated soil column under steady flow. It can be described by 1D advection–diffusion equation

$$\frac{\partial C}{\partial t} + \frac{\partial (u_x C)}{\partial x} = \frac{\partial}{\partial x}\left(D_x \frac{\partial C}{\partial x} \right) \tag{34}$$

DOI: 10.1002/fld

with the following boundary conditions

$$\begin{aligned} C(x,t) &= C_0, \quad x=0 \\ \partial C/\partial x &= 0, \quad x=L \end{aligned} \tag{35}$$

where $C_0=0.001\,\mathrm{kg/m}$ and $L=0.3048\,\mathrm{m}$ with dispersion coefficient $D_x=1.075\times10^{-7}\,\mathrm{m^2/s}$ and velocity $u_x=4.23\times10^{-6}\,\mathrm{m/s}$. This is the same as Problem 1a by Wexler [21] who gives the following analytical solution:

$$C(x,t)=C_0\left[1-2\exp\left(\frac{xu_x}{2D_x}-\frac{u_x^2t}{4D_x}\right)\sum_{i=1}^{\infty}\frac{\beta_i\sin\left(\dfrac{\beta_i x}{L}\right)\exp\left(-\dfrac{\beta_i^2D_xt}{L^2}\right)}{\beta_i^2+\left(\dfrac{u_xL}{2D_x}\right)^2+\dfrac{u_xL}{2D_x}}\right] \tag{36}$$

where β_i are the roots of the equation,

$$\beta\cot\beta+\frac{u_xL}{2D_x}=0 \tag{37}$$

In the computation, the rectangular lattices comprising 40 grids in the x direction and 10 in the y direction are used with $\Delta x=0.00762\,\mathrm{m}$ and $\Delta y=0.01524\,\mathrm{m}$ and $\Delta t=76.2\,\mathrm{s}$. In order to investigate the effect of relaxation time on solutions, several values of $\tau=0.6$, 1.0, 1.1, 1.2 and 1.5 were used to solve the problem. The results are shown in Figure 2. It is clearly seen from the figure that the results for $1.0\leqslant\tau\leqslant1.2$ are almost the same and otherwise different. Consequently, the use of a value in the range of $1.0\leqslant\tau\leqslant1.2$ can produce solution, which is independent of the relaxation time, and hence a value in the range or close to it is generally chosen as the relaxation time in numerical computations. The results with $\tau=1.1$ at different time are depicted in Figure 3 and

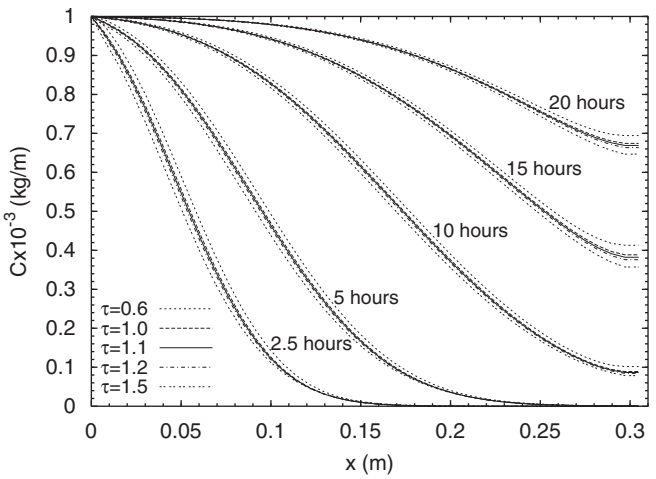

Figure 2. 1D test: effect of τ on solutions.

DOI: 10.1002/fld

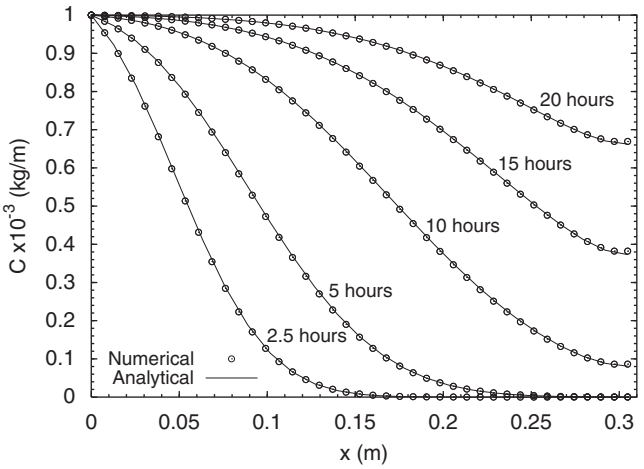

Figure 3. 1D test: concentrations change with time.

compared with the analytical solutions from Equation (36), demonstrating an excellent agreement between them. This confirms the accuracy of the proposed model.

3.2. 1D point source transport with constant velocity

The second test is the transport of 1D point source in infinite domain. This is a classic problem in environmental hydraulics. It is governed by the same advection–diffusion equation as Equation (34) with the following boundary conditions:

$$C(x,t)=0, \quad x=\pm\infty \tag{38}$$

which has an exact solution,

$$C(x,t)=\frac{C_0}{\sqrt{4\pi D_x t}}\exp\left[-\frac{(x-u_x t)^2}{4D_x t}\right] \tag{39}$$

A point source with $C_0=1\,\mathrm{kg/m}$ at $x=10\,\mathrm{m}$ which is discharged into the channel with $L=400\,\mathrm{m}$ at the start. The diffusion coefficient is $D_x=0.01\,\mathrm{m}^2/\mathrm{s}$ and the velocity $u_x=0.01\,\mathrm{m/s}$. This is the same problem investigated by Zhang *et al.* [12].

For comparison, the same computation parameters as that used in the reference [12] were used, i.e. the lattices comprise 400 points in the x direction and 4 in the y direction with $\Delta x=1\,\mathrm{m}$ and $\Delta y=1\,\mathrm{m}$ as well as $\tau=1.1$ and $\Delta t=0.1\,\mathrm{s}$. The numerical results at $t=10000\,\mathrm{s}$ and $t=30000\,\mathrm{s}$ are compared with the exact solution (39) and shown in Figure 4, from which there is an excellent agreement between them, which confirms the accuracy of the proposed model. However, the predictions in the reference [12] is overshooted in the peak regions and undershooted in the front regions of the two profiles.

DOI: 10.1002/fld

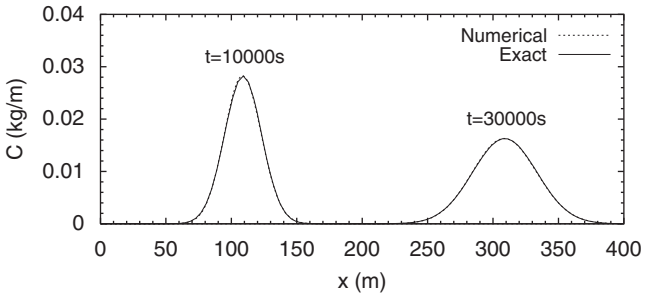

Figure 4. 1D point source: comparison with the exact solution.

3.3. 2D solute transport with finite-width solute source

The third test is that migration of chloride ion in landfill leachate through a narrow, relatively thin, valley-fill aquifer, which are governed by the following 2D advection–diffusion equation

$$\frac{\partial C}{\partial t}+\frac{\partial (u_x C)}{\partial x}+\frac{\partial (u_y C)}{\partial y}=\frac{\partial}{\partial x}\left(D_x\frac{\partial C}{\partial x}\right)+\frac{\partial}{\partial y}\left(D_y\frac{\partial C}{\partial y}\right) \tag{40}$$

subject to the boundary conditions

$$C(x,t)=\begin{cases} C_0, & x=0 \text{ and } y_1\leqslant y\leqslant y_2 \\ 0, & x=0 \text{ and } y<y_1 \text{ or } y>y_2 \end{cases} \tag{41}$$

and

$$\begin{aligned} &\partial C/\partial x=0, \quad x=L \\ &\partial C/\partial y=0, \quad y=0 \text{ or } y=W \end{aligned} \tag{42}$$

in which $W=900\,\text{m}$ is the aquifer width, $y_1=121.92\,\text{m}$, $y_2=609.9\,\text{m}$, $L=1500\,\text{m}$, $C_0=1\,\text{kg/m}^2$, the dispersion coefficients are $D_x=2.150533\times10^{-4}\,\text{m}^2/\text{s}$, $D_y=6.4516\times10^{-5}\,\text{m}^2/\text{s}$, $u_x=3.527777\times10^{-6}\,\text{m/s}$ and $u_y=0$. This is the same as Problem 6 by Wexler and its analytical solution is [21],

$$\begin{aligned} C(x,y,t)=C_0\sum_{n=0}^{\infty}L_n P_n\cos(\eta y)\left\{\exp\left[\frac{x(u_x-\beta)}{2D_x}\right]\text{erfc}\left[\frac{x-\beta t}{2\sqrt{D_x t}}\right]\right. \\ \left.+\exp\left[\frac{x(u_x+\beta)}{2D_x}\right]\text{erfc}\left[\frac{x+\beta t}{2\sqrt{D_x t}}\right]\right\} \end{aligned} \tag{43}$$

in which

$$L_n=\begin{cases} \frac{1}{2}, & n=0 \\ 1, & n>0 \end{cases} \tag{44}$$

$$P_n=\begin{cases} (y_2-y_1)/W, & n=0 \\ [\sin(\eta y_2)-\sin(\eta y_1)]/(n\pi), & n>0 \end{cases} \tag{45}$$

DOI: 10.1002/fld

$$\eta = n\pi / W, \quad n = 0, 1, 2, 3, \ldots \tag{46}$$

$$\beta = \sqrt{u_x^2 + 4\eta^2 D_x D_y} \tag{47}$$

In this test, 60×60 rectangular lattices were used, i.e. $\Delta x = 25\,\text{m}$ and $\Delta y = 15\,\text{m}$, together with $\tau = 0.9$ and $\Delta t = 500\,000\,\text{s}$ in the simulation. The results at 1500 days and 3000 days are presented here for comparisons with the analytical solutions from Equation (43). The contours of the concentrations are shown in Figures 5 and 6, where the analytical solutions are also depicted, showing very good agreement. The comparisons of the central profiles with analytical solutions are plotted in Figure 7, which also present the results from the square lattice. All of these again show excellent agreement.

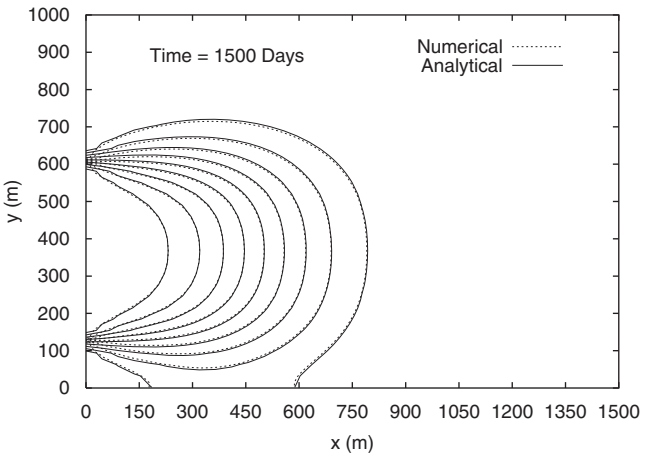

Figure 5. 2D test: contours of concentration at 1500 days.

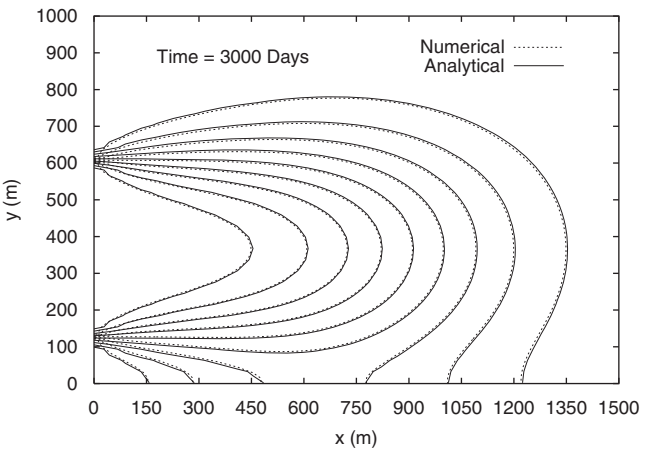

Figure 6. 2D test: contours of concentration at 3000 days.

DOI: 10.1002/fld

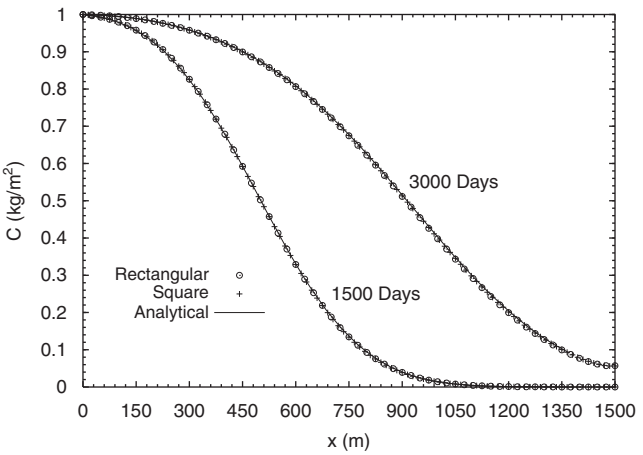

Figure 7. 2D test: comparisons of central profiles.

3.4. 2D shear dispersion

The final test is a problem with longitudinal dispersion, which is a typical problem related to solute transport under shear flows in environmental engineering. A 2D problem with non-uniform profile for velocity distribution in transversal direction is considered here. The problem is governed by the same equation as Equation (40) with the periodic boundary conditions at inlet and outlet, and the following boundary condition along the transversal direction:

$$\frac{\partial C}{\partial y}=0, \quad y=0 \text{ or } y=W \tag{48}$$

In this test, $L=400\,\text{m}$, $W=10\,\text{m}$, $D_x=0.01\,\text{m}^2/\text{s}$, $D_y=0.01\,\text{m}^2/\text{s}$ and $u_y=0$. The following parabolic velocity profile is assumed for u_x in the transversal direction throughout the channel in the simulation

$$u_x(x,y,t)=U_0\left[1-\left(\frac{2y-W}{W}\right)^2\right] \tag{49}$$

where $U_0=0.1\,\text{m/s}$. A contaminant with $C_0=1\,\text{kg/m}^2$ is injected uniformly across the cross-section at $x=6.5\,\text{m}$ at the same time. According to the environmental hydraulics, there is a longitudinal dispersion due to non-uniformity of velocity profile in transversal direction. Since the channel is quite narrow and the full transversal diffusion is soon achieved after a short time, the longitudinal dispersion will dominate the transport. In the computations, $\tau=1$ was used.

In order to demonstrate the potential of the proposed model, first of all, different lattices in flow directions, i.e. 800×20, 1200×20, 1600×20, 2000×20, 2400×20, 2800×20 and 3000×20, were used. The results are shown in Figure 8, indicating that the lattice number in longitudinal direction has strong effect on the solution and the results based on lattice number which is not less than 2800 can produce lattice-independent solution for the problem.

Then, different lattices in transversal direction, i.e. 3000×10, 3000×20 and 3000×40, were used. The results are plotted in Figure 9, which clearly shows that the lattice number in transversal

DOI: 10.1002/fld

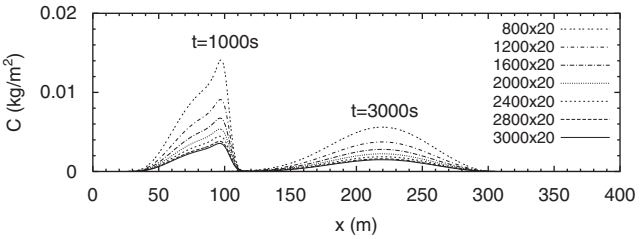

Figure 8. Shear dispersion: central profiles based on different lattices in longitudinal direction.

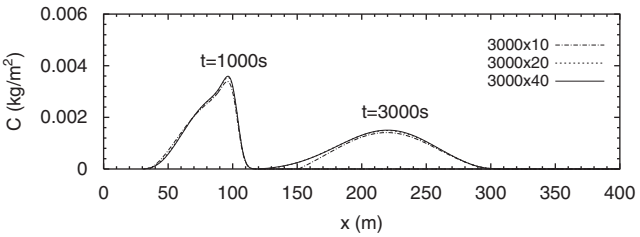

Figure 9. Shear dispersion: central profiles based on different lattices in transversal direction.

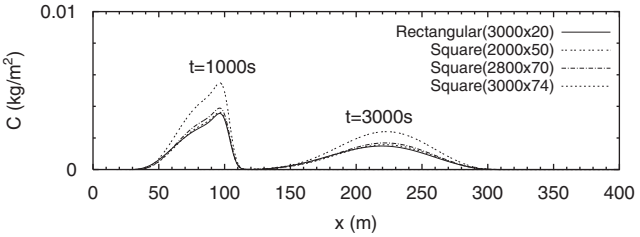

Figure 10. Shear dispersion: comparisons of central profiles between rectangular and square lattices.

direction has much less effect on the solution. Thus, the results based on lattice number larger than or equal to 20 will provide almost the same solutions for the problem.

Next, the results based on different square lattices, 2000×50, 2800×70 and 3000×74, were also obtained and compared with that from the rectangular lattices of 3000×20, which are depicted in Figure 10. From the figure, it follows that the results with square lattices of 2800×70 can provide lattice-independent solution at the similar accuracy to that from the rectangular lattices of 3000×20. However, the simulation time for the former is at least triple that of the latter as listed in Table I, suggesting that the proposed model is more efficient than that on a square lattice.

Finally, the problem is further solved with the finite difference method and the results are compared with that from the proposed method in Figure 11. This again confirms the accuracy of the proposed model. The contours of the shear dispersion are plotted in Figure 12, demonstrating the typical patterns of shear dispersion with time.

DOI: 10.1002/fld

Table I. Comparisons of simulation time.

Solutions at time	1000 s	3000 s
Square lattice (2800×70)	9 min 48 s	33 min 10 s
Rectangular lattice (2800×20)	2 min 52 s	10 min 43 s
Square lattice (3000×74)	11 min 36 s	39 min 23 s
Rectangular lattice (3000×20)	3 min 16 s	11 min 20 s

Note: The calculations were carried out on a PC with CPU of 1.8 GHz.

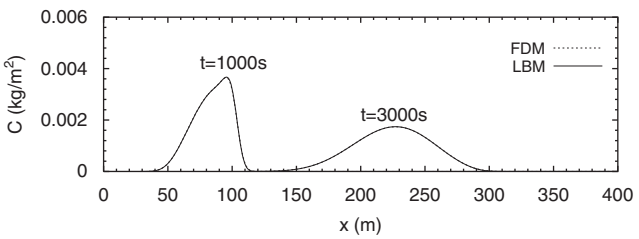

Figure 11. Shear dispersion: comparisons central profiles between the lattice Boltzmann method (LBM) and the finite difference method (FDM).

Figure 12. Shear dispersion: contours at $t = 0$ s, 1000 s and 3000 s (the line source at $t = 0$ s is exaggerated for clarity in the above figure).

4. CONCLUSIONS

A lattice Boltzmann method for solute transport suitable for both rectangular and square lattices is presented in this paper. The basic feature of the method is that it is formulated on the basis of a natural extension of the local equilibrium distribution functions on square lattice to rectangular lattice without any modification to either the lattice Boltzmann equation or the calculation procedure. It then preserves a simple procedure and the same efficiency as that for a standard lattice Boltzmann method on a square lattice. It has shown that the use of 5-velocity lattice makes the model more efficient in simulations at the similar accuracy to that based on 9-velocity lattice for a 2D problem. This provides the present method with potential capability when it is applied to a large-scale practical problems for solute transport. The method has been validated with four tests. It is simple, accurate and conservative.

DOI: 10.1002/fld

APPENDIX A

A.1. 3D model

A 3D lattice Boltzmann model for solute transport on a 7-speed cuboid lattice is essentially the same as that for 2D model described in Section 2 with the following four modifications:

1. The local equilibrium distribution function f_α^{eq} is

$$f_\alpha^{\mathrm{eq}}=\begin{cases}\left(1-\dfrac{\lambda_z e_x^2 e_y^2+\lambda_y e_x^2 e_z^2+\lambda_x e_y^2 e_z^2}{e e_x e_y e_z}\right)C, & \alpha=0\\ \left(\dfrac{1}{2}\dfrac{e_y e_z}{e_x e}\lambda_x+\dfrac{e_{\alpha i}u_i}{2e_x^2}\right)C, & \alpha=1 \text{ and } 3\\ \left(\dfrac{1}{2}\dfrac{e_x e_z}{e_y e}\lambda_y+\dfrac{e_{\alpha i}u_i}{2e_y^2}\right)C, & \alpha=2 \text{ and } 4\\ \left(\dfrac{1}{2}\dfrac{e_x e_y}{e_z e}\lambda_z+\dfrac{e_{\alpha i}u_i}{2e_z^2}\right)C, & \alpha=5 \text{ and } 6\end{cases} \tag{A1}$$

   where

$$e_z=\frac{\Delta z}{\Delta t},\quad e=\frac{\Delta x+\Delta y+\Delta z}{3\ \Delta t} \tag{A2}$$

   in which Δz is the lattice size in the z direction.

2. λ_i is expressed as

$$\lambda_i=\frac{eD_i}{\Delta t(\tau-\frac{1}{2})e_x e_y e_z} \tag{A3}$$

3. The stability conditions are

$$\tau>\frac{1}{2},\quad \Delta t<\frac{(\tau-\frac{1}{2})\Delta x^2\Delta y^2\Delta z^2}{D_x\Delta y^2\Delta z^2+D_y\Delta x^2\Delta z^2+D_z\Delta x^2\Delta y^2} \tag{A4}$$

4. The vector of the particle speed $\mathbf{e}_\alpha$ is defined by

$$\mathbf{e}_\alpha=\begin{cases}(0,0,0), & \alpha=0\\ e_x\left[\cos\dfrac{(\alpha-1)\pi}{2},\sin\dfrac{(\alpha-1)\pi}{2},0\right], & \alpha=1,3\\ e_y\left[\cos\dfrac{(\alpha-1)\pi}{2},\sin\dfrac{(\alpha-1)\pi}{2},0\right], & \alpha=2,4\\ e_z[0,0,\cos(\alpha-5)\pi], & \alpha=5,6\end{cases} \tag{A5}$$

DOI: 10.1002/fld

REFERENCES

1. Chen S, Doolen GD. Lattice Boltzmann method for fluid flows. *Annual Review of Fluid Mechanics* 1998; **30**:329–364.
2. Xu YS, Liu Y, Xu XZ, Huang GX. Lattice Boltzmann simulation on molten carbonate fuel cell performance. *Journal of the Electrochemical Society* 2006; **153**(3):A607–A613.
3. Zhou JG. A lattice Boltzmann model for groundwater flows. *International Journal of Modern Physics C* 2007; **18**(6):973–991.
4. Ni YS, Liu CF, Lin DS. A lattice Boltzmann model of statistical evolution of microvoids. *Materials Science and Engineering A—Structural Materials Properties Microstructure and Processing* 2006; **423**(1–2):79–83.
5. Ghai SS, Kim WT, Amon CH, Jhon MS. Transient thermal modeling of a nanoscale hot spot in multilayered film. *Journal of Applied Physics* 2006; **99**(8):08F906.
6. van der Sman RGM. Finite Boltzmann schemes. *Computers and Fluids* 2006; **35**:849–854.
7. Rohde M, Kandhai D, Derksen JJ, van den Akker HEA. A generic, mass conservative local grid refinement technique for lattice-Boltzmann schemes. *International Journal for Numerical Methods in Fluids* 2006; **51**(4): 439–468.
8. van der Sman RGM, Ernst MH. Convection–diffusion lattice Boltzmann scheme for irregular lattices. *Journal of Computational Physics* 2000; **160**:766–782.
9. van der Sman RGM. Diffusion on unstructured triangular grids using lattice Boltzmann. *Future Generation Computer Systems* 2004; **20**(6):965–971.
10. Chew YT, Shu C, Niu XD. A new differential lattice Boltzmann equation and its application to simulate incompressible flows on non-uniform grids. *Journal of Statistical Physics* 2002; **107**(1–2):329–342.
11. Wu HR, He YL, Tang GH, Tao WQ. Lattice Boltzmann simulation of flow in porous media on non-uniform grids. *Progress in Computational Fluid Dynamics* 2005; **5**(1–2):97–103.
12. Zhang XX, Bengough AG, Crawford JW, Young IM. A lattice BGK model for advection and anisotropic dispersion equation. *Advances in Water Resources* 2002; **25**(1):1–8.
13. Flekkoy EG. Lattice Bhatnagar–Gross–Krook models for miscible fluids. *Physical Review E* 1993; **47**:4247–4257.
14. Yeo IW. Solute dispersion in rock fractures by non-Darcian flow. *Geophysical Research Letters* 2001; **28**(20): 3983–3986.
15. Rasin I, Succi S, Miller W. A multi-relaxation lattice kinetic method for passive scalar diffusion. *Journal of Computational Physics* 2005; **206**:453–462.
16. Skordos PA. Initial and boundary conditions for the lattice Boltzmann method. *Physical Review E* 1993; **48**: 4823–4842.
17. Zhou JG. *Lattice Boltzmann Methods for Shallow Water Flows*. Springer: Berlin, 2004.
18. Bhatnagar PL, Gross EP, Krook M. A model for collision processes in gases. I: small amplitude processes in charged and neutral one-component system. *Physical Review* 1954; **94**:511–525.
19. Dawson SP, Chen S, Doolen GD. Lattice Boltzmann computations for reaction–diffusion equations. *The Journal of Chemical Physics* 1993; **98**:1514–1523.
20. van der Sman RGM, Ernst MH. Convection–diffusion lattice Boltzmann scheme for irregular lattices. *Journal of Computational Physics* 2000; **160**:766–782.
21. Wexler EJ. *Analytical Solutions for One-, Two-, and Three-Dimensional Solute Transport in Ground-water Systems with Uniform Flow*. United State Government Printing Office: U.S.A., 1992.

DOI: 10.1002/fld